Microstructure and Composition of Electromagnetically-Characterized $YBa_2Cu_3O_{7-\delta}$ Grain Boundaries

Susan E. Babcock,[*,**] Na Zhang,[**] Yufei Gao,[†,††,‡] Xue Yu Cai,[**]
Debra L. Kaiser,[‡‡] David C. Larbalestier,[*,**] and Karl L. Merkle[††,‡]

[*]Department of Materials Science and Engineering and
[**]Applied Superconductivity Center
University of Wisconsin, Madison, WI USA
[†]Science and Technology Center for Superconductivity and
[††]Materials Science Division, Argonne National Laboratory,
Argonne, IL 60439
[‡‡]Ceramics Division, National Institute for Standards
and Technology, Gaithersburg, MD USA

[‡]This work was supported by the National Science Foundation (DMR88-09854) through the Science and Technology Center for Superconductivity (YG) and by the U.S. Department of Energy, Offices of Basic Energy Sciences-Materials Science (KLM) under contract No. W-31-109-Eng.-38.

Manuscript submitted for the Proceedings of the 2nd Tokai University International Workshop on Superconductivity, Hawaii, October 1991. To be published in The Journal of Advanced Science (Japan).

Proc. 2nd Tokai University International Workshop on Superconductivity (October 1991). To appear in The Journal of Advanced Science (Japan)

MICROSTRUCTURE AND COMPOSITION OF ELECTROMAGNETICALLY-CHARACTERIZED $YBa_2Cu_3O_{7-\delta}$ GRAIN BOUNDARIES

Susan E. BABCOCK,[1,2] Na ZHANG,[2] Yufei GAO,[3] Xue Yu CAI,[2] Debra L. KAISER,[4]
David C. LARBALESTIER[1,2] and Karl L. MERKLE[3]
[1]Department of Materials Science and Engineering and [2]Applied Superconductivity Center,
University of Wisconsin, Madison WI, USA;
[3]Science and Technology Center for Superconductivity and Materials Science Division,
Argonne National Laboratory, Argonne IL, USA;
[4]Ceramics Division, National Institute for Standards and Technology, Gaithersburg MD, USA.

ABSTRACT

The electrical character (flux-pinning, Josephson junction, or resistive) of the grain boundaries in approximately twenty flux-grown $YBa_2Cu_3O_{7-\delta}$ bicrystals was determined in previous studies. A selection of these same bicrystals now have been thinned for study by transmission and scanning transmission electron microscopy. High-spatial resolution imaging and analytical techniques reveal microstructural differences among these boundaries that are consistent with their diverse electrical characteristics. The observations offer preliminary insight into some of the features that control the grain boundary superconducting properties and re-emphasize the very fine scale on which the grain boundary electrical character is determined.

Key words: $YBa_2Cu_3O_{7-\delta}$, Grain Boundary, Microstructure, Critical Current Density, Electron Microscopy.

1. INTRODUCTION

The original thin-film bicrystal studies of Dimos et al.[1] strongly indicated that all high-angle grain boundaries in $YBa_2Cu_3O_{7-\delta}$ are intrinsically weak-linked and exhibit the transport critical current characteristics (J_{ct}) of a Josephson junction. More recent investigations of individual grain boundaries in both bulk-scale bicrystals[2] and textured thin films[3] have shown that the J_{ct} properties of high-angle grain boundaries can vary in important ways. Specifically, high-angle grain boundaries with J_{ct} behavior characteristic of a flux pinning mechanism have been discovered in flux-grown bicrystals, and evidence for inhomogeneous electrical properties within individual Josephson junction-like grain boundaries has been found for thin-films. These results are encouraging for applications of $YBa_2Cu_3O_{7-\delta}$ because they suggest that the grain boundary J_{ct} properties may be manipulated by processing. However, further process engineering of polycrystalline materials can be conducted in an informed way only when the microstructural origin of the observed behavior is understood. This paper describes high-spatial resolution investigations of the microstructure and composition of $YBa_2Cu_3O_{7-\delta}$ grain boundaries of known and fundamentally different electromagnetic character.

2. METHODS AND MATERIALS

The bicrystals are produced by the flux method in which $YBa_2Cu_3O_{7-\delta}$, BaCuO, and CuO are melted together in a gold crucible.[4] During a carefully controlled cool-down, sharply-faceted single crystals

form from the melt. As these crystals grow, they frequently impinge and expel the melt phase from the new interface to form grain boundaries that are free of large-scale second phase. The superconducting properties of the grain boundaries in approximately 20 bicrystals of this type have now been measured directly.[2,5] A current lead and a voltage contact are placed on each side of the boundary and the critical current is measured for applied fields ranging from a few milli-tesla to 7T at 77K. The characteristic signatures of Josephson junction- and flux-pinning-limited electrical transport appear in the field dependence of J_{ct}. Resistive measurements of the superconducting transition temperature (T_c) are also made. To date, the following four different types of grain boundaries have been identified on the basis of their superconducting properties:[5,6]

(1) flux-pinning;

(2) Josephson junction;

(3) parallel flux-pinning and Josephson junction paths; and

(4) resistive at $T \geq 4.2K$.

At least one high-angle bicrystal of each type has been found.

For the present studies, samples for transmission and scanning transmission electron microscopy (TEM and STEM) were prepared from bicrystals of types 2 and 4. High-resolution electron microscopy (HREM) images of the grain boundary region were obtained for each bicrystal. Energy-dispersive x-ray spectroscopy (EDXS) performed in a high-spatial-resolution STEM (~3 nm interaction volume) was used to analyze the grain boundary composition for a Josephson-junction-type grain boundary. Light microscopy and diffraction-contrast TEM imaging were used to investigate the larger-scale microstructure and crystallographic parameters of the grain boundary.

3. RESULTS AND DISCUSSION

3.1. Grain Boundary Microstructure

Figures 1 and 2 show diffraction contrast images of a Josephson junction-like and a resistive high-angle grain boundary, respectively. The grain boundary microstructure appears to be the same in both bicrystals at this scale (~5 nm), even though their properties are fundamentally different. Both grain boundaries are nearly in the symmetrical tilt position in the electron-transparent region of the TEM sample. At the grain boundary the twin boundaries of one grain align with those of the other grain. Twin matching of the type described in detail by Gayle and Kaiser[7] is also observed in the light micrographs of these samples. Geometrical models of grain boundary structure predict that the symmetrical tilt position corresponds to an energy minimum for a given crystal misorientation. Relaxation into twin-matched microstructures also suggests that these boundaries have assumed atomic structures that correspond to local energy minima. Finally, the macroscopic misorientation relationships measured for these bicrystals suggest that they may be considered to contain near-low-Σ boundaries. 43°[001] is very close to a Σ=29 misorientation relationship (43.6° [001]) for the parent tetragonal unit cell, and the 26°[001] is somewhat close to the Σ=17 misorientation relationship at 28.1° [001]. Evidence that these low-Σ misorientations correspond to low-energy structures is found in the literature.[8] Thus, several of the frequently cited macroscopic expressions of these grain boundaries' energies suggest that they might have: (a) short-period structures that are relatively free of grain boundary microstructural defects and (b) concomitant special (and perhaps desirable) electrical properties. Therefore, on the basis of the boundary crystallography alone, it is somewhat surprising that these two bicrystals have fundamentally different electromagnetic characteristics. (Note that the (001) planes of one crystal are parallel to those of the other crystal and approximately perpendicular to the grain boundary plane for both bicrystals studied here.)

In addition to their similar boundary crystallography, like-appearing local diffraction contrast (small, dark spots) is also observed along both

boundaries. The origin of this irregular contrast has yet to be determined conclusively, but its presence suggests that both boundaries are microstructurally inhomogeneous on a finer scale than can be resolved by diffraction-contrast imaging.

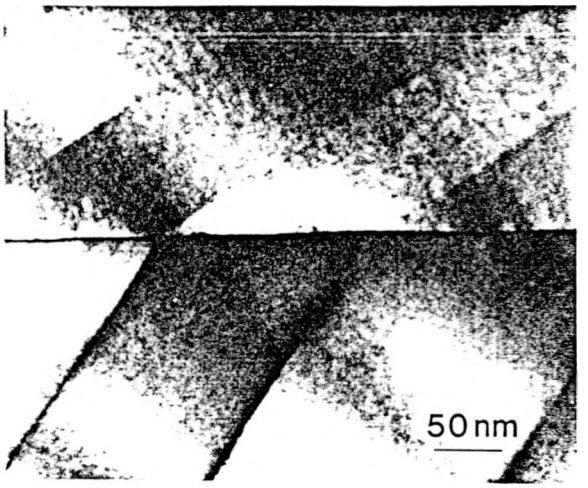

Fig.1. Diffraction-contrast TEM image of a Josephson-junction-like grain boundary. The bicrystal misorientation relationship is ~26° [001]. The grain boundary is nearly in the (410) symmetrical tilt position at this location.

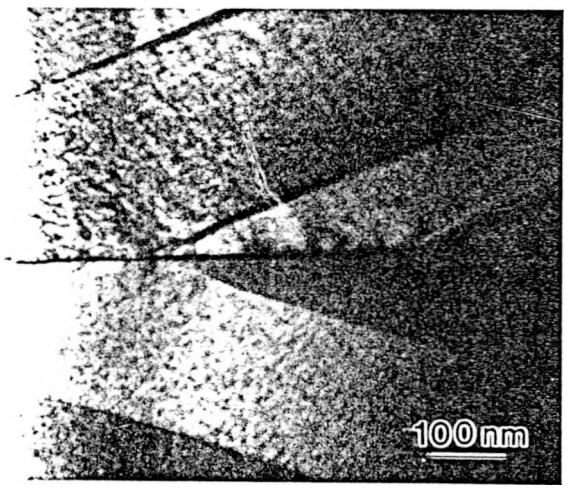

Fig.2. Diffraction-contrast TEM image of a resistive (at 4.2 K) with a grain boundary misorientation relationship of ~ 43° [001]. The grain boundary plane is nearly the (520) symmetrical tilt position at this location.

The likeness of the microstructural features found in Figures 1 and 2 implies that diffraction-contrast imaging offers little information about the source for the electrically-different layer that *must* exist at these two grain boundaries. However, high-resolution imaging and compositional analysis of these grain boundaries has provided some insight into the origins of their electrical properties.

HREM images of the 26° [001] and 43° [001] grain boundaries are shown in Figs. 3 and 4, respectively. A most striking difference in the boundary microstructures is observed in these two images. The resistive grain boundary (Fig. 4) is clearly wet by a 1-3 nm thick layer of second phase whose thickness is relatively inhomogeneous on the scale of the high-resolution image. Although a substantial lattice

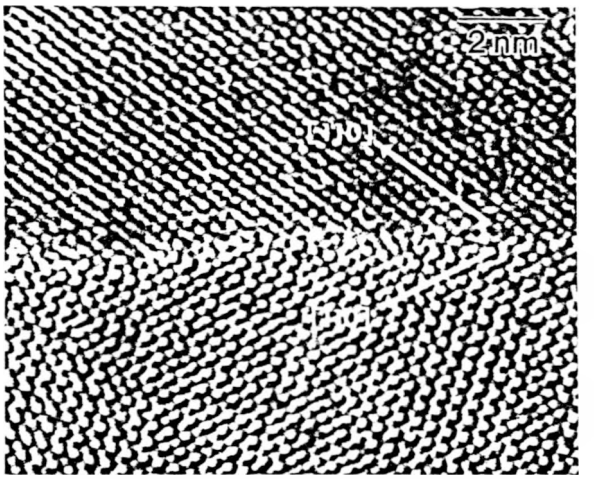

Fig.3. HREM image of the Josephson-junction-like grain boundary shown in Fig. 1.

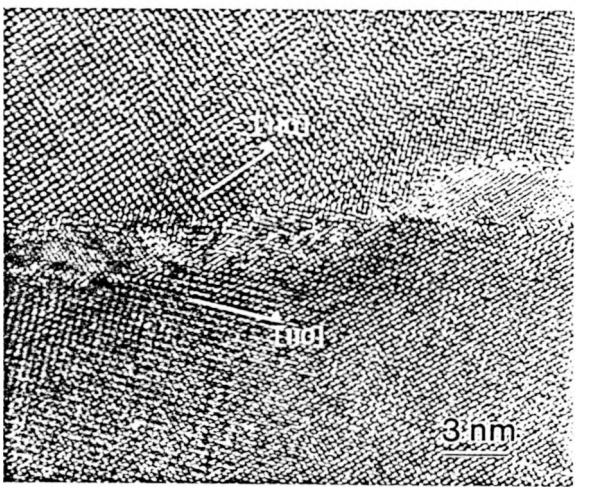

Fig.4. HREM image of the resistive grain boundary shown in Fig. 2.

mismatch between the intergranular phase and the $YBa_2Cu_3O_{7-\delta}$ and concomitant strain is evident, the intergranular phase appears to prefer a specific orientation relationship with the $YBa_2Cu_3O_{7-\delta}$.

In contrast, the Josephson junction boundary (Fig. 3) is free of second phase and the structure of each grain appears to remain intact to within about 0.5 nm of the other grain. Thus, the structural width of the boundary is approximately 0.5 nm. This width must be compared to the superconducting coherence length (ξ) in the (001) plane, which is estimated at 1.5 to 2.5 nm. The highly distorted region associated with the boundary core thus appears to be considerably shorter than ξ in the direction of the current. This comparison suggests that factors in addition to the structural width of the grain boundary core (e.g., composition changes, elastic strain, atomic mismatch of the conducting planes, etc.) contribute to the boundary's electrical properties.

3.2. Grain Boundary Composition

Figs. 5 and 6 contain composition information deduced from EDXS for the Josephson junction grain boundary shown in Figs. 1 and 3. For the analysis the grain interiors were presumed to have the stoichiometric 1:2:3 cation composition. This assumption is justified by the data, because each in-grain measurement falls within the range of uncertainty of all of the other in-grain measurements. It also implies, however, that the method only reveals composition differences, not absolute concentrations. Because the oxygen content was not constant in time-resolved measurements, it was fixed at 16.38 wt. % (δ=0.1) for the analysis. The average gold concentration was assumed to be 2.02 wt. %, in accordance with explicit determinations of the gold content of single crystals produced by the flux-growth method.[9]

The data in Fig. 5 suggest that the grain boundary is richer in copper than the grain interiors. This result is consistent with the observed copper richness of the grain boundary cores in sintered materials[10] and the suggested presence of Cu-O at primary grain boundary dislocation cores in thin-film samples.[11] Assuming reasonable estimates of the thickness of the segregation zone (approximately one unit cell dimension, ~0.3-0.5 nm) and the diameter of the x-ray-signal-producing zone (~3-5 nm), the grain boundary cation composition required to produce the observed composition change is in the range of 1:2:4 to 1:2:6. Unfortunately, the 124

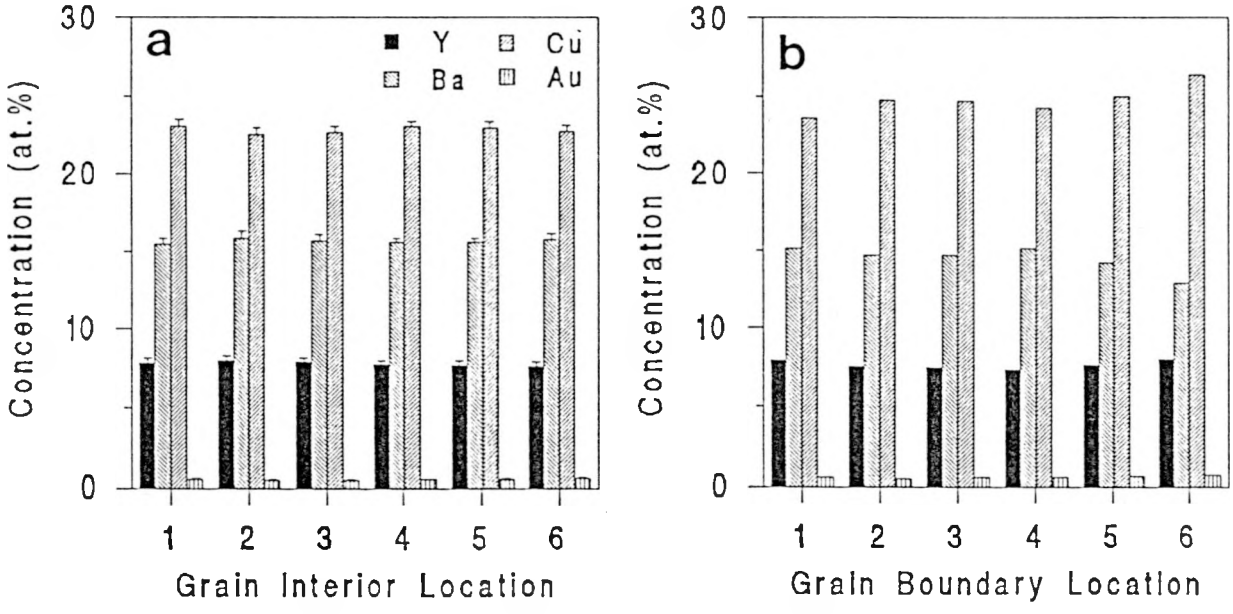

Fig.5. Cation composition at several sites (b) in the grain boundary of Figs. 1 and 3 and in the (a) adjacent grains. Error bars represent 3σ confidence as deduced from the x-ray counts .

and 247 phases cannot be detected by high-resolution imaging in this projection (beam aligned along [001] of each grain). A similar estimate suggests that the thickness of the pure CuO oxide layer that would produce the observed increase in Cu concentration is ~0.08 nm. This thickness is inconsistent with the presence of a *homogeneous* layer of CuO such as might be produced by CuO primary grain boundary dislocation cores and, therefore, suggests a different dislocation core composition for nominally stoichiometric material.[11] However, it remains possible that discrete Cu-O like regions exist in the boundary, such as might arise due to facet junction dislocations or grain boundary defects.

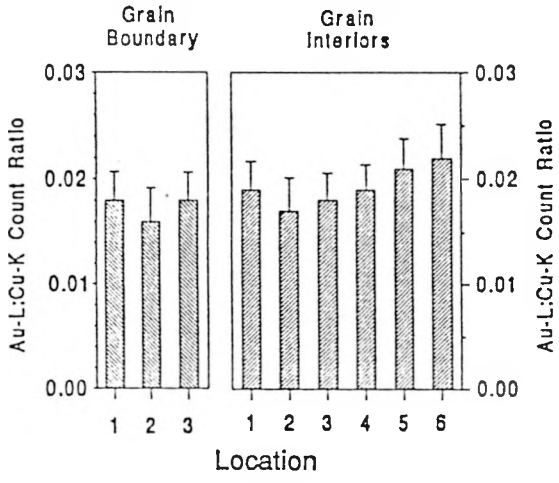

Fig.6. Comparison of Au to Cu characteristic x-ray intensity for positions within grain boundary to locations within the grains. Au impurities substitute on Cu sites in flux-grown single crystals.

X-ray diffraction experiments have shown that Au substitutes for ~7% of the chain-site copper atoms in this material.[9] Figure 6 shows x-ray data that are pertinent to the gold concentration at the grain boundary. These data indicate that Au does not segregate to the grain boundaries in these bicrystals. However, the small weight fraction of Au present implies limited sensitivity to local *changes* in the gold concentration. On the basis of the current data, it was estimated that a doubling of the Au concentration at the grain boundary relative to the grain interiors would be just detectable by the EDXS method used here. However, a doubling of the Au concentration would still correspond to a rather small fraction of a monolayer coverage at the grain boundary (approximately one gold atom for every seven $YBa_2Cu_3O_{7-\delta}$ unit cells along the boundary). It was therefore concluded that significant gold segregation to the grain boundary did not occur in this sample. This conclusion is supported by the similar grain boundary resistivity values that are obtained for thin-film[3] and flux-grown bicrystals.[5]

4. CONCLUDING COMMENTS

The coupled microstructural and electromagnetic characteristic of grain boundaries described here show that the details of the grain boundary superconducting properties are indeed determined on the scale of the superconducting coherence length. Undoubtedly linked to the fine scale on which the electron transport mechanism is determined, fundamentally different superconducting properties are observed for boundaries with similar crystallography and grain boundary microstructure. High-spatial resolution imaging and composition determinations have revealed microstructural features that are consistent with the measured electrical properties of the boundaries from which they are obtained, but these techniques have yet to pinpoint the fundamental sources for the different superconducting properties. A principal goal of our on-going studies is to discover and manipulate the microstructural features that promote flux-pinning character at some high-angle grain boundaries and Josephson junction character at others.

REFERENCES

[1]D. Dimos, P. Chaudhari, and J. Mannhart, Phys. Rev. B **41** (190) 4038.

[2]S.E. Babcock, X.Y. Cai, D.L. Kaiser, and D.C. Larbalestier, Nature **347** (1990) 167.

[3]S.E. Russek, D.K. Lathrop, B.H. Moeckly, R.A. Buhrman, D.H. Shin, and J. Silcox, Appl. Phys. Lett. **57** (1990) 1155..

[4]D.L. Kaiser, F. Holtzberg, B.A. Scott, and T.R. McGuire, Appl. Phys. Lett. **51** (1987) 1040.

[5]D.C. Larbalestier, S.E. Babcock, X.Y. Cai, M.B. Field, Y. Gao, N.F. Heinig, K.L. Merkle, L.K.

Williams, and N. Zhang, To appear in Physica C (1991).

[6]S.E. Babcock, in "Structures/Properties Relationships for Interfaces," ASM, To appear in 1991

[7]F.W. Gayle and D.L. Kaiser, J. Mater. Res., 6 (1990) 908.

[8]D.A. Smith, M.F. Chisholm, and J. Clabes, Appl. Phys. Lett. 53 (1988) 2344.

[9]W. Wong-Ng, F.W. Gayle, D.L. Kaiser, S.F. Watkins, and F.R. Fronczek, Phys. Rev.B. 41 (1990) 4220.

[10]S.E. Babcock and D.C. Larbalestier, Appl. Phys. Lett. 55 (1989) 393 and references cited within.

[11]Y. Gao, K.L. Merkle, G. Bai, H.L.M. Chang and D.J. Lam, Physica C 174 (1991) 1.

ACKNOWLEDGMENTS

This work is sponsored by the NSF Materials Research Group Program (DMR-8911332). Y. Gao is supported by the NSF Science and Technology Center for Superconductivity (DMR88-09854). K.L. Merkle is supported by the U.S. Department of Energy (BES-Materials Science, W-31-109-ENG-38). The use of the H9000 high-resolution electron microscope at Northwestern University, Evanston IL, is gratefully acknowledged.